

The ULO Shelyak Spectrograph

Report on bench tests conducted during 2011 June-July

Stephen Boyle

1st November 2012

1 Introduction

In 2011 June a Shelyak Instruments Lhires III spectrograph was delivered to the University of London Observatory (ULO), with the intention of eventually using the spectrograph on the 12-inch Celestron telescope mounted in the east dome of the new building. This report describes the results of bench tests carried out on the Shelyak Spectrograph during 2011 June and July. Shelyak Instruments provides information on its Lhires III spectrograph on its company web site; see Ref.1.

2 Bench tests: 2011 June 16; spectra of the neon lamp.

Spectra of the instrument's internal neon calibration lamp were obtained at various wavelength ranges. Wavelength is selected by using a robustly constructed micrometer screw. I obtained images of the neon arc at micrometer settings between 12.00 mm and 17.80 mm, at intervals of either 0.20 mm or 0.40 mm; all settings were made from below. Images were captured using an ST-8 CCD camera and recorded as FITS image files. The length of the imaging surface parallel to the direction of dispersion of the spectrograph was 1530 pixels. The cooling mechanism of the ST-8 camera did not function; the background count was nevertheless low enough to allow usable images of neon lines to be obtained. The high resolution grating was used for these tests, the one one incorporated in the 1200 grooves mm^{-1} grating module supplied with the spectrograph. The 35 μm —the widest available—was used. Some results of these tests are presented in Table 2.

Initial impressions formed while operating the spectrograph:

- The body of the spectrograph is very light in weight. This is obviously helpful, in that the spectrograph will likely contribute little disturbance to the balance of the telescope, but an inescapable consequence is that the spectrograph feels somewhat flimsy.
- The neon lamp is selected by turning, all the way anticlockwise, a knob that is very stiff.
- Access to an alternative lamp (e.g., Argon) would provide more lines in the blue region of the spectrum.
- The method of adjusting collimator focus is a little clumsy, and the lack of a focus scale makes determination of best focus position a matter of judging by eye.

Observations of Neon emission lines:

- Neon lines were recorded. Exposure times required ranged from about 10 minutes at short wavelengths (corresponding to low readings on the micrometer), down to 5 seconds in the red region of the spectrum.

Table 1: Measurements made from a sample of the neon arcs exposed on 2011 June 16. ‘HWHM’ is the half-width at half-maximum, in pixels, of a neon emission line chosen at random in each frame. As a check of how well the measurements may be reproduced, two exposures were made at 16.60mm.

Micrometer reading (mm)	Start wavelength (Å)	Recip. linear disp. (Å pixel ⁻¹)	Quadratic term (10 ⁻⁶ Å pixel ⁻²)	HWHM (pixel)
16.20	5527.751	0.1406	-2.8	3.3
16.60	5658.417	0.1379	-2.8	3.3
16.60	5658.264	0.1384	-3.0	2.6
17.00	5787.715	0.1350	-2.8	2.6
17.40	5915.090	0.1324	-2.9	2.6
17.80	6043.333	0.1295	-3.0	2.6

- The spectrum obtained at micrometer reading 17.80 mm was extracted first, and calibrated for wavelength, using the Figaro package. The wavelength range of the calibrated spectrum was 6044 Å to 6234 Å. The reciprocal dispersion was determined to be 0.13 Å pixel⁻¹.
- With the 1200 grooves mm⁻¹ grating in place, an increase in the micrometer reading of 0.40 mm increases the central wavelength of the exposed spectrum by about 130 Å, producing a reasonable overlap in the wavelength coverage of exposures made at successive micrometer settings.

3 Bench tests: 2011 June 29; the entrance slits

Four entrance slits are available; these are in the form of rulings in the opaque coating of a square glass window positioned in front of the circular entrance aperture of the spectrograph. The slits have fixed widths of 15, 19, 23 and 35 μm; the width of each slit is indicated by a two-digit number engraved to its left, as shown in Figure 3 of this report. The desired slit is selected via the following procedure:

- 3.1 Remove (using a 2.5 mm metric Allen key) the two screws that hold the aluminium base plate of the window to the black anodised support that is firmly attached to the body of the spectrograph;
- 3.2 Lift the base plate clear of the support;
- 3.3 Grasp the window frame from below and pull it out of the base plate;
- 3.4 Rotate the window and place it upon the anodised support, so that the desired slit lies in front of the circular entrance aperture;
- 3.5 Carefully place the base plate back on top of the window;
- 3.6 Very cautiously, use the Allen key to screw the base plate to the black anodised support. There is evident danger of chipping, or breaking the slit window at this stage.

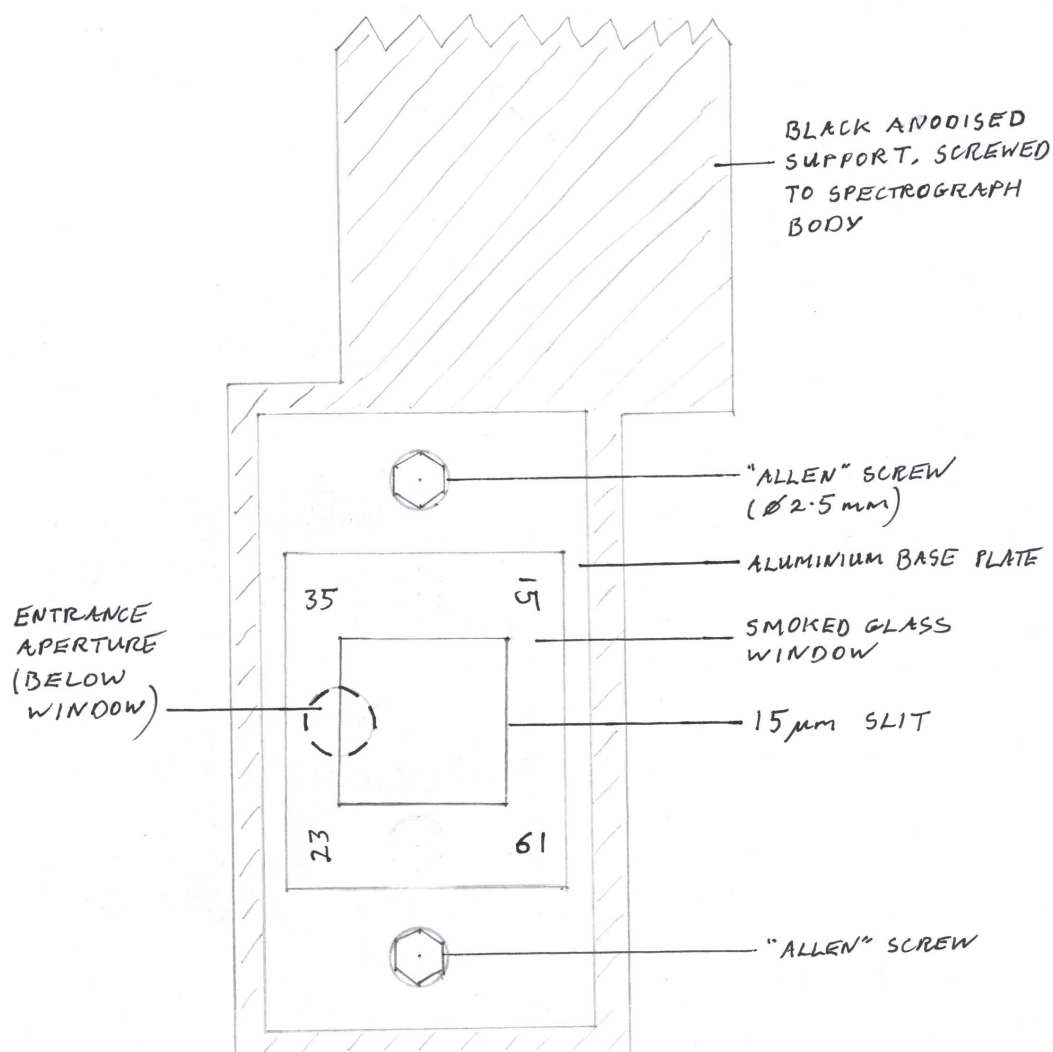


Figure 1: The Shelyak spectrograph: selection of the slit. In this illustration, the 23 μm slit lies in front of (above) the entrance aperture.

Having gained some confidence that I could alter the entrance slit as required, I proceeded to investigate the effect of slit width upon measured line width. I set the micrometer screw gauge

Table 2: The effect of slit width upon the measured width of the Ne I ($\lambda 6074 \text{ \AA}$) line recorded during a 4-second exposure.

Slit width (μm)	Line centre (pixel)	Line FWHM (pixel)	Integrated count (ADU $\times 10^6$)
15	1240.59 ± 0.06	4.47 ± 0.18	1.61 ± 0.05
19	1199.87 ± 0.05	4.77 ± 0.15	2.26 ± 0.05
23	1248.71 ± 0.04	4.98 ± 0.13	2.47 ± 0.05
35	1222.83 ± 0.04	6.12 ± 0.11	4.40 ± 0.06

to 17.400 mm, and took one exposure of 4 seconds with each slit. The exposed spectra were each summed over columns 460 to 560 of the CCD. For each extracted spectrum, the line centre, the full-width at half-maximum (FWHM) and the integrated ADU count in the Ne I ($\lambda 6074 \text{ \AA}$) line were estimated from the best-fit gaussian curve determined by the DIPSO and ELF programs. The resulting effect of the width of the entrance slit upon measured spectrum line width is documented in Table 3. From these results we note that:

- 3.7 It was essentially impossible to avoid altering the position of a spectrum line on the CCD while the slit. This is probably not surprising, given the manual, involved process required to change the slit.
- 3.8 The measured FWHM of an emission line invariably increased with as the slit width increased. A straight line fitted to the relevant data in Table 2 produced the following relationship between line FWHM (w_l) and slit width (w_s):

$$\frac{w_l}{\text{pixel}} = (3.18 \pm 0.06) + (0.083 \pm 0.006) \frac{w_s}{\mu\text{m}}.$$

- 3.9 The signal integrated under an emission line increased with as the slit width increased. This result, like that in 3.8, is as expected.

4 Bench tests: 2011 July 1; collimator focus

Collimation of the spectrograph is achieved by turning a screw. Unfortunately there is no scale on the screw, a situation that does not aid the recovery of an optimum collimation position. However, it proved to be reasonably easy to recover the position of near optimum focus by visual inspection of arc lines displayed on a monitor.

There follows a little more detail of the procedure that I followed while investigating the collimator focus. The wavelength micrometer screw gauge was set to 17.400 mm, so as to view the prominent Ne I ($\lambda 6074 \text{ \AA}$) line. The narrowest slit available, at 15 μm -wide, was used. Four exposures were obtained, with the collimator screw rotated anticlockwise (as viewed from the end of the barrel that faced the CCD camera) by approximately $\frac{1}{4}$ of a turn between each exposure. A further exposure was obtained, with the focus optimised by visual inspection of the emission line displayed upon a monitor.

Table 3: The effect of collimator focus setting upon the measured width of the Ne I ($\lambda 6074 \text{ \AA}$) line recorded during five test exposures of 4-seconds each. Focus setting is expressed as the number of anticlockwise turns from an arbitrary starting position. 'By eye' refers to the results of optimising the focus by visual inspection of the lines displayed on a monitor, with no reference to the number of turns of the screw.

Screw Turns anticlockwise	Line centre (pixel)	Line FWHM (pixel)	Integrated count ($\text{ADU} \times 10^6$)
0	1233.03 ± 0.07	4.47 ± 0.21	1.57 ± 0.05
1/4	1216.509 ± 0.012	3.38 ± 0.03	1.80 ± 0.01
1/2	1261.037 ± 0.017	4.14 ± 0.04	1.65 ± 0.01
3/4	1261.12 ± 0.19	8.5 ± 0.4	1.62 ± 0.08
'By eye'	1218.133 ± 0.014	3.30 ± 0.04	1.82 ± 0.02

The results of the collimation tests are presented in Table 4. From these it seems evident that good collimation can, with a little practice, be obtained by eye. Clearly, one turn of the collimation screw is sufficient to bring the image of a bright emission line from a very evident poor focus, passing through a point of optimum focus, to poor focus again.

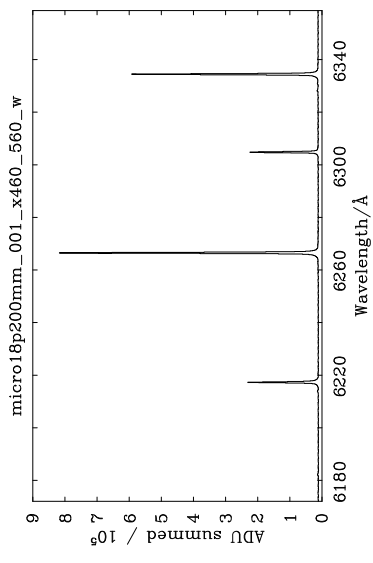
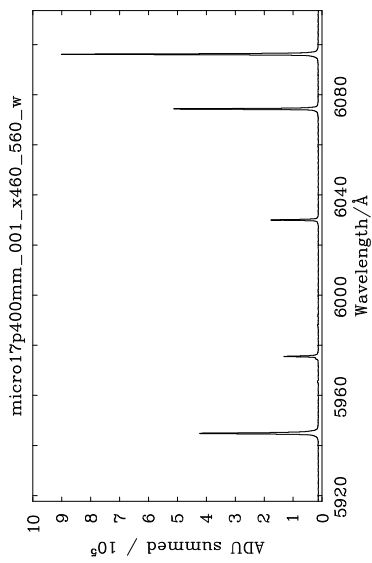
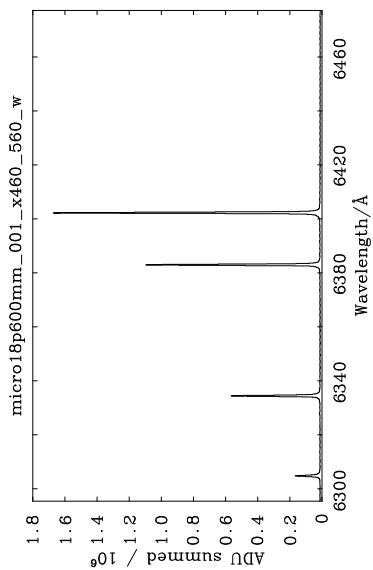
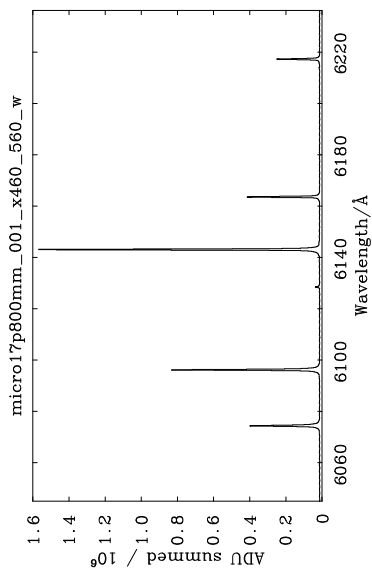
5 Bench tests: 2011 July 6; arc atlas

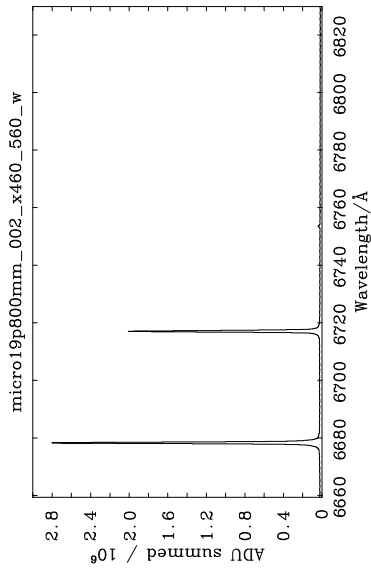
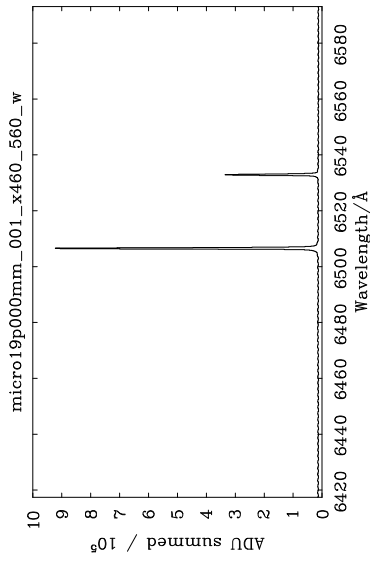
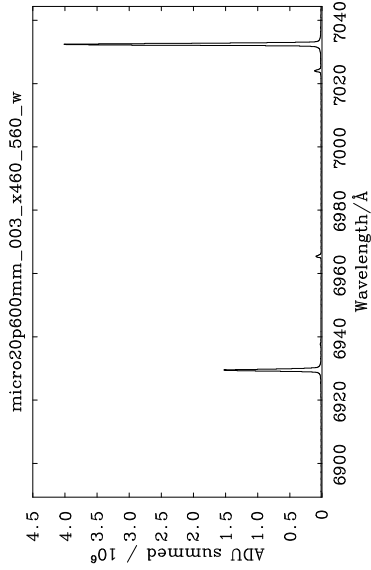
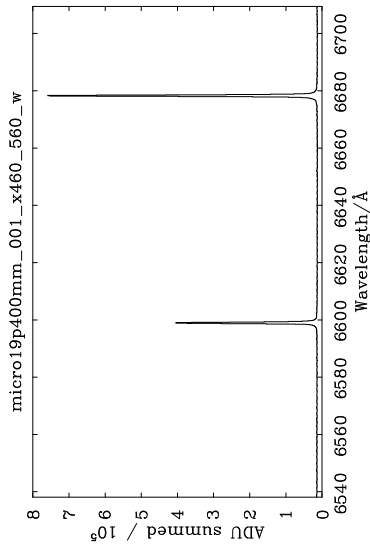
The 2400 lines mm^{-1} grating was used to generate the atlas (that appears a page or two hence) of emission lines produced by the Shelyak spectrograph's Neon calibration lamp. The setting of the micrometer gauge used to produce each spectrum appears in the heading of each panel, e.g. a setting of 20.200 mm was used to produce the spectrum headed "micro20p200mm".

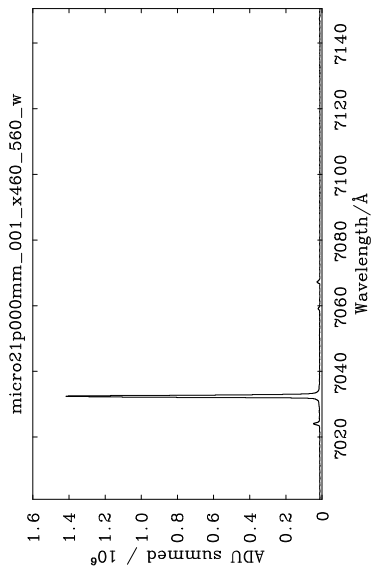
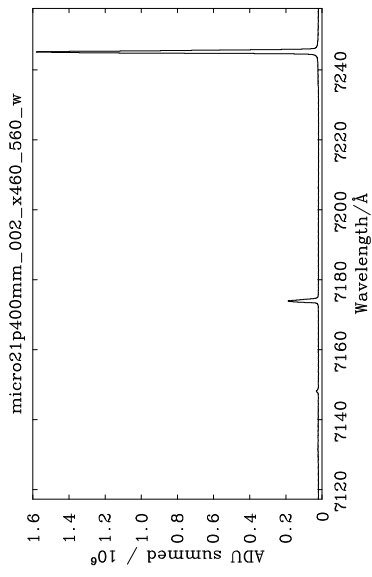
6 Work to be done: 2012-2013

- The arc atlas needs to be extended to shorter wavelengths.
- Collimator focus has been found to depend on wavelength, but the lack of a scale on the collimation screw renders it impossible to establish a best-fit function of focus position as a function of wavelength. However, it should be possible to determine the FWHM at *best* focus for a range of wavelengths, by visual inspection.
- Perform on-telescope tests of wavelength stability with respect to flexure. Tests need to be made with the telescope pointing at several different positions, and at the start and end of a long period of tracking.
- Perform on-telescope tests of wavelength stability with respect to ambient temperature in the dome.

*
5349.21 NeI
5355.30 NeI
5360.012 NeI
5372.31 NeI
5374.975 NeI
5400.562 NeI
5412.66 NeI
5418.56 NeI
5433.65 NeI
5494.41 NeI
5562.769 NeI
5652.57 NeI
5656.659 NeI
5662.547 NeI
5689.817 NeI
5719.225 NeI
5748.298 NeI
5760.59 NeI
5764.418 NeI
5804.449 NeI
5811.42 NeI
5820.155 NeI
5828.91 NeI
5852.488 NeI
5881.895 NeI
5902.464 NeI
5944.834 NeI
5965.474 NeI
5975.534 NeI
6029.997 NeI
6074.338 NeI
6096.163 NeI
6128.451 NeI
6143.063 NeI
6163.594 NeI
6217.281 NeI
6266.495 NeI
6304.789 NeI
6334.428 NeI
6382.991 NeI
6402.247 NeI
6506.528 NeI
6532.882 NeI
6598.953 NeI
6652.09 NeI
6678.277 NeI
6717.043 NeI
6929.468 NeI
7024.051 NeI
7032.413 NeI
7059.109 NeI
7173.939 NeI
7245.167 NeI
*







7 Reference

1. Shelyak Instruments, description - LhiresIII, date unknown. Available on-line at:
http://www.shelyak.com/dossier.php?id_dossier=46
(last accessed: 1st November 2012).